# We are IntechOpen, the world's leading publisher of Open Access books Built by scientists, for scientists

**4,800**
Open access books available

**122,000**
International authors and editors

**135M**
Downloads

Our authors are among the

**154**
Countries delivered to

**TOP 1%**
most cited scientists

**12.2%**
Contributors from top 500 universities

CLARIVATE ANALYTICS BOOK CITATION INDEX INDEXED

WEB OF SCIENCE™

Selection of our books indexed in the Book Citation Index in Web of Science™ Core Collection (BKCI)

## Interested in publishing with us?
## Contact book.department@intechopen.com

Numbers displayed above are based on latest data collected.
For more information visit www.intechopen.com

# 2

# Crystallization on Self Assembled Monolayers

Michal Ejgenberg and Yitzhak Mastai
*Bar Ilan University*
*Israel*

## 1. Introduction

Over the past two decades, self assembled monolayers (SAMs) (Love *et al.*, 2005; Smith *et al.*, 2004; Ulman, 1996) have been extensively studied due to their many applications in various fields such as electrochemistry (Eckerman *et al.*, 2010), biosensors (Nyquist *et al.*, 2000), protein separation (Chun and Stroeve, 2002) and enantiomer separation (Mastai, 2009). SAMs are organic assemblies formed by the adsorption of molecules from solution or from the gas phase onto the surfaces of solids. These molecules spontaneously organize into highly ordered, crystalline (or semicrystalline) two dimensional films. The molecules composing the SAMs adsorb to the surface through a "headgroup", a functional group with a high affinity for the solid surfaces. Two of the most widely studied systems of SAMs are alkanethiols adsorbed on metals, including gold, silver and platinum and alkylsilane chains formed on silicon dioxide surfaces, including glass and mica. In these cases, the "headgroups" are thiols, which have a high affinity for metal surfaces and silanes, which have a high affinity for silicon-dioxide surfaces. SAMs have become so popular since they offer a unique combination of physical properties that allow fundamental studies of interfacial chemistry, solvent molecule interactions and self-organization. Their well-ordered arrays and ease of functionalization make them ideal model systems in many fields.

One of the important advantages of SAMs is that they can be prepared in the laboratory by dipping the desired substrate in the required solution for a specified time followed by thorough washing with the same solvent and drying, often using a jet of dry nitrogen. Gas-phase evaporation of the adsorbate can also form good monolayers, although structural control is difficult. Several factors affect the formation and packing density of the self assembled monolayers including the solvent, temperature, nature of adsorbate, adsorbate concentration and the nature and roughness of the substrate. SAM substrates range from planar surfaces to highly curved surfaces (which will not be discussed here). The most common planar substrates for alkanethiol SAMs are thin films of metals supported on flat surfaces, such as glass, silica wafers and mica. These substrates can be easily prepared using methods like physical vapor deposition (PVD) and chemical vapor deposition (CVD). In some cases, an additional layer of titanium or chromium between the solid and the metal is needed in order to improve the adhesion between them. The composition of the thin films (grain size, etc.) is affected by the properties of the metal used (for example, melting point), the solid surface roughness and the experimental conditions. This, in turn, affects the organization and density of the SAM. The most common alkylsilane substrates are silicon dioxide surfaces such as glass, which are usually pre-treated with sulfuric acid.

The self assembled adsorbate has a great influence on the SAM outcome and can be tailored according to the desired SAM properties. The molecule used can possess a number of functional groups in addition to the molecule's headgroup. These functional groups can be distributed within the monolayer interior and located at the terminus of the molecule. Manipulation of the monolayer interior affects its degree of order and how easily electrons are conducted through it. For example, the molecular chain length and the steric crowding of the organic groups affect the density of the organic layer and the tilt angle of the molecule away from the surface normal. In general, longer chains and less robust organic groups yield denser, more organized SAMs, allowing high degrees of van der Vaals interactions (and in some cases, hydrogen bonds) with the neighboring molecules. The molecular constituent exposed at the SAM surface is critical to the SAM's interfacial properties. It affects the surface's general hydrophobic/hydrophilic character, adhesive properties and reactivity. In addition, it determines the surface interaction with other molecular species that come in contact when placed on the surface of the SAM.

SAMs are of prime technological interest, as the presence of molecules chemically bound to the surface renders the properties of the modified interface (i.e., wetting, conductivity, adhesion, and chemistry) to be entirely different than those of the bare substrate. The incorporation of functional moieties such as chromophores, electroactive groups, or molecules that can bond within the SAM (i.e., covalent cross-linking between adjacent molecules or non-covalent hydrogen bonding) enable capabilities in sensing, electron transfer, molecular recognition, and other areas (Smith *et al.*, 2004).

This review will focus on the use of SAMs in crystallization processes. We will begin with a short introduction on crystallization on SAMs. Then, we will review the latest advances in crystallization on patterned SAM's and effects of SAMs on crystal morphology and crystal polymorphism. This chapter will also include a description of chiral SAMs and their role in enantioselective crystallization.

## 2. Crystallization on SAMs

Crystallization refers to the formation of solid crystals from a solution, melt or more rarely, directly from gas. Crystallization consists of two processes – nucleation and crystal growth. Nucleation is the formation of small clusters of molecules. These clusters may re-dissolve in the crystallizing solution or go on to become a crystal, depending on their size. Beyond a critical size, they are stable and form crystal nuclei. Crystal growth refers to the subsequent addition of molecules to the formed nuclei. The nucleation can be homogenous, occurring spontaneously or heterogenous, induced by foreign particles such as dust particles or vessel walls. Primary nucleation occurs in the absence of crystals in solution whereas secondary nucleation occurs on seeds or existing crystals present in the crystallizing solution.

The ability to control crystallization is a critical requirement in many technologies such as in the food, pharmaceutical and chemical industries. Crystallization parameters such as particle size, particle shape, particle morphology and polymorph selectivity determine the crystal properties and uses. The solution concentration, crystallization time, crystallization temperature, solvent and crystallization vessel all have an effect on the crystal parameters. In the past few decades, researchers have been busy searching for new ways to control crystallization. Self assembled monolayers are showing great promise in this field. The

SAMs interact with the crystallizing molecules and thus, affect their organization, ultimately affecting the crystallization outcome. SAMs have been reported to affect crystal orientation, morphology, polymorphism and crystal size. The interaction between SAMs and molecules in solution has usually been rationalized on the basis of hydrogen bonding and/or strong ionic interactions.

### 2.1 Effects on crystal orientation

During crystallization, the SAM constituent exposed at the SAM surface interacts with molecules present in the crystallizing solution. These interactions are specific and in turn, can cause the stabilization of specific crystal faces. When this happens, the crystals grow in a specific orientation, causing changes in crystal morphology. Many researchers have reported specific crystal orientation on SAMs, brought about by interactions of the crystallizing molecules with SAMs.

For example, Lee *et al*. employed SAMs of rigid thiols on gold surfaces in order to investigate the effects of interfacial molecular recognition on nucleation and growth of L-Alanine and DL-Valine crystals (Lee *et al.*, 2002). L-alanine crystallizes from water in the orthorhombic space group $P2_12_12$ (a=6.025Å, b=12.324Å and c=5.783Å), with bipyramidal morphology, dominated by the {020}, {120}, {110} and {011} growth forms (Figure 1).

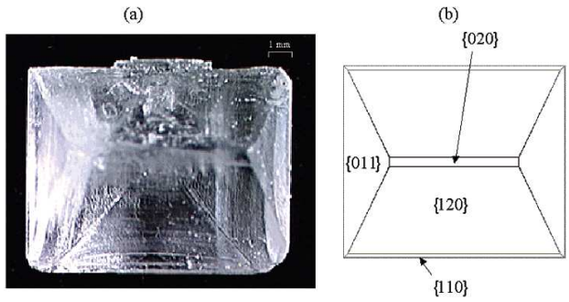


Fig. 1. L alanine crystal grown from aqueous solution. (Lee *et al.*, 2002)

In order to examine the effect of the SAMs on L-Alanine crystallization, L-Alanine was crystallized from solutions and also onto a variety of rigid SAMs of thiols: 4'-methyl-4-mercaptobiphenyl, 4'-hydroxy-4-mercaptobiphenyl and 4-(4-mercaptophenyl) pyridine. Powder X-ray diffraction patterns and interfacial angle measurements of the L-alanine crystals are shown in Figure 2. In methyl-terminated SAMs, L-alanine selectively nucleated on the (020) plane on the SAM surface while on the OH-terminated SAMs, L-alanine nucleated on an unobserved (200) side face. In both cases, the area of each crystal face was substantially larger than the other faces on the crystal. Crystallization of L-alanine on 4-(4-mercaptophenyl) pyridine resulted in the (011) face as the plane corresponding to nucleation. The preferential interaction was explained on the basis of hydrogen bonding between the pyridine surface and the amino and methyl groups protruding out of the (011) plane. Figure 2 reveals that L-alanine crystals nucleating on SAM surfaces crystallize in an orthorhombic space group with similar unit cell dimensions. However, the functionalized SAMs have an effect on the nucleating plane and ultimately, on L-alanine crystal growth.

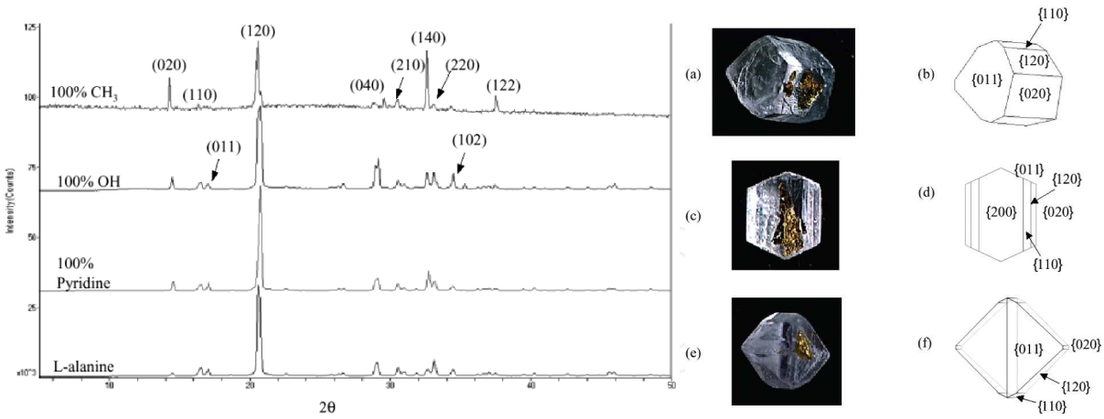


Fig. 2. X-ray diffraction spectra of L alanine nucleated on functional SAMs compared with L alanine crystallized from aqueous solution (left) and crystallographic images and morphology of L-alanine crystallized on (a,b) 4′-methyl-4-mercaptobiphenyl SAMs, (c,d) 4′-hydroxy-4-mercaptobiphenyl SAMs and (e,f) 4-(4-mercaptophenyl) pyridine SAMs – (right). (Lee *et al.*, 2002)

DL-Valine crystallizes in the monoclinic space group $P2_1/c$ with unit cell dimensions (a=5.21Å, b=22.10Å, c=5.41Å and β=109.2°). In aqueous solution, DL-valine crystallizes as hexagonal platelets dominated by a slow-growing (020) flat face with (100), (002) and (202) side faces. DL-valine was crystallized on 4′-methyl-4-mercaptobiphenyl, 4′-hydroxy-4-mercaptobiphenyl and 4-(4-mercaptophenyl) pyridine. On the pyridine and OH-terminated thiols, DL-valine crystals nucleated from the flat (020) plane, whereas in methyl terminated SAMs, the fast growing (100) face was the nucleating plane and the hexagonal platelet crystals were oriented perpendicular to the SAM surface (Figure 3). Again, the surface chemistry of the SAMs led to different interfacial interactions and thus oriented the crystallization of amino acids. In both cases, hydrogen bonding was responsible for the epitaxial crystallization of the amino acid on the monolayer substrates. Molecular modelling studies were also undertaken to examine the molecular recognition between the monolayer and the crystallographic planes and were in good agreement with the experimental results.

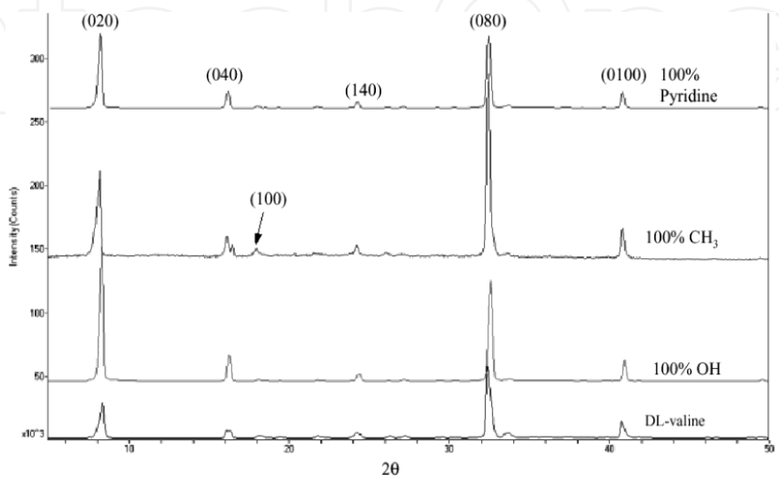

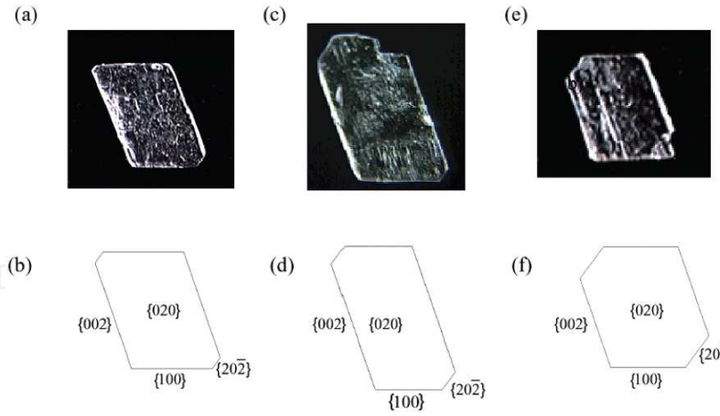


Fig. 3. X-ray diffraction spectra of DL valine nucleated on functional SAMs compared with DL valine crystallized from aqueous solution (top) and crystallographic images and morphology of DL valine crystallized on (a,b) 4-(4-mercaptophenyl) pyridine SAMs, (c,d) 4′-hydroxy-4-mercaptobiphenyl SAMs and (e,f) 4′-methyl-4-mercaptobiphenyl SAMs – (bottom). (Lee *et al.*, 2002)

An additional example for the effect of SAMs on crystallization can be demonstrated in the work of Aizenberg and co-workers, who studied the growth of oriented calcium carbonate crystals on X-terminated alkanethiol SAMs ($HS(CH_2)_nX$) (Aizenberg *et al.*, 1999). The SAMs were terminated with a variety of functional groups ($X=CO_2^-$, $SO_3^-$, $PO_3^{2-}$, OH, $N(CH_3)_3^+$,$CH_3$) and two different metal support films were used – Ag and Au. The calcium carbonate crystals were characterized by a variety of techniques – optical microscopy, SEM with image analysis and X-ray diffraction. Their results showed that SAMs terminated in acidic functionalities were found to induce nucleation more effectively than control surfaces of bare metal films, whereas SAMs terminated in $CH_3$ or slightly basic $N(CH_3)_3$ actually inhibited their nucleation. The orientation of the crystals was highly homogeneous for each surface and depended on the functional group exposed at the SAM surface. The authors achieved a very high level of control over the orientations of the crystals. They were able to selectively nucleate calcite from six crystallographic planes. This was the first time that calcite had been grown in such a variety of orientations in an artificially controlled system.

### 2.2 Effects on polymorphism

Polymorphism is the ability of a molecule to crystallize in more than one packing arrangement. Polymorphs (Chieng et al., 2011) may possess significantly different structural and physical properties and therefore polymorphism has broad practical implications in solid state chemistry, materials science and pharmacology. Many methods have been developed to control polymorphism including tailor made additives (Yokota et al., 2006), surfactants (Garti and Zour, 1997) and varying solvents and temperature (Weissbuch et al., 2005). Recently, self assembled monolayers have also been shown to control crystal polymorphism.

Hiremath *et al.* applied SAM templates in order to control the polymorphism of 1,3-bis(*m*-nitrophenyl) urea (MNPU – Figure 4). (Hiremath *et al.*, 2005) Previously studied, MNPU was found to have at least three different polymorphs - α, β and γ. The polymorphs are visually

distinguishable, but often crystallize concomitantly from aqueous ethanol solutions. The crystal structures of the α and β polymorphs were first reported by Etter et al (Etter *et. al*, 1988, 1990, as cited in Hiremath *et al*., 2005). Bernstein *et al.* (Bernstein *et al*., 2005, as cited in Hiremath *et al*., 2005) obtained the crystal structure of the γ phase and also discovered a previously unknown anhydrous δ phase.

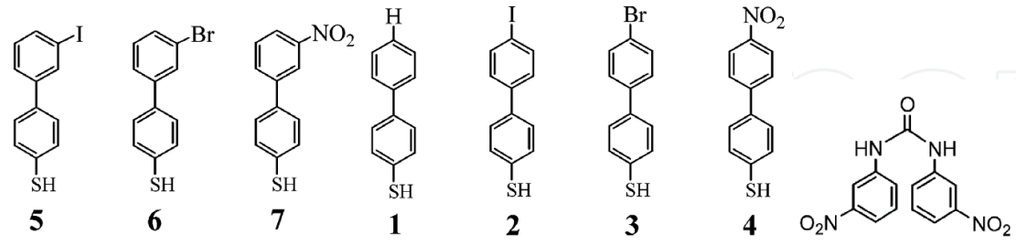


Fig. 4. MNPU (right) and biphenyl thiol molecules used in the biphenyl thiol SAMs (1-7) – (left). (Hiremath *et al*., 2005)

Initially, Hiremath *et al.* obtained the pure polymorph phases by varying solvents and temperature. The α-MNPU was obtained from crystallization in ethanol at 60°C, β-MNPU was obtained from crystallization in ethyl acetate at room temperature. The γ form was obtained by re-crystallization of the α or β forms in 95% ethanol. Then, MNPU was crystallized on a variety of biphenyl thiol SAMs (Figure 4) and two types of control surfaces: bare gold substrates and 1-pentanethiol, 1-octanethiol and 1-dodecanethiol SAMs. The biphenyl thiols were chosen for two reasons – their close packing affords a more perpendicular molecular alignment at the surface (smaller tilt angles) and the slightly larger size of the 2D lattice dimensions makes them potentially more compatible with typical unit cell dimensions. The crystallizations were conducted in saturated ethanol or ethyl acetate solutions of MNPU at room temperature or 60°C. The results obtained from the crystallizations are summarized in Table 1. Crystals of MNPU only appeared on SAMs 1-3. No crystallization of MNPU was observed on SAMs 4-7 or on the control surfaces. SAMs of 1, 2 and 3 were each found to serve as selective nucleating templates for a single MNPU phase. Crystals of α-MNPU formed on monolayers of 1, β-MNPU grew selectively on 2 and γ-MNPU grew on 3. The crystallizations were repeated numerous times and the results were always consistent. The resultant crystal form obtained was independent of the solvent or temperature conditions explored. In addition, the crystals grown on SAMs 1-3 all adopted preferred orientations with respect to the SAM templates, illustrating the importance of the interface in the nucleation process. The observed orientations were rationalized on the basis of two-dimensional lattice matching, complementary functional group interactions and dipole moments across the SAM/crystal interface.

The work of Dressler and Mastai provides an additional example of polymorphism control by SAMs. Dressler and Mastai crystallized the metastable α-L-Glutamic acid on L-Phenylalanine SAMs (L-AAPP, Figure 5) (Dressler and Mastai, 2007). L-Glutamic acid is known to form two polymorphs – the metastable α-form and the stable β-form. It was previously shown that the stable β-form emerges from the metastable α-crystals through a kinetic process. It was also shown that the α-polymorph converts rapidly to the β-form at 45°C, but at ca. 15°C, the conversion process is very slow and almost nonexistent, so that the

α-polymorph is obtained exclusively. Dressler and Mastai demonstrated that the α-form can be obtained at room temperature, without the need for crystallization at low temperatures.

| SAM | initial solute phase | solvent | temp (°C) | growth |
|---|---|---|---|---|
| **1** | α, *β*, or *γ* or any combination of phases | ethanol or ethyl acetate | 25 or 60 | α |
| **2** | α, *β*, or *γ* or any combination of phases | ethanol or ethyl acetate | 25 or 60 | *β* |
| **3** | α, *β*, *γ* or any combination of phases | ethanol or ethyl acetate | 25 or 60 | *γ* |
| **4**, **5**, **6**, **7**, bare gold, or alkanethiol controls | α, *β*, *γ* or any combination of phases | ethanol or ethyl acetate | 25 or 60 | none |

Table 1. Crystal of MNPU grown on SAMs 1-7 including the initial solution phase, solvent and temperature crystallization parameters. (Hiremath *et al.*, 2005)

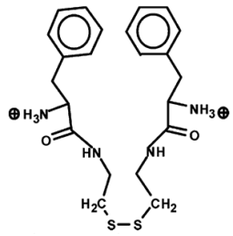


Fig. 5. L-AAPP (Dressler and Mastai, 2007)

Substrates for SAM preparation were prepared by vacuum deposition of thin gold films onto glass slides. The gold substrates were then immersed in 2mM L-AAPP ethanolic solutions overnight in order to receive the L-AAPP SAMs. L-AAPP was chosen as the molecule for self assembly since L-phenylalanine has already been shown to promote the stabilization of the α-form of L-glutamic acid in solution. In order to examine the effect of the SAMs on L-glutamic acid crystallization, a series of crystallization experiments were performed on the surfaces and in solutions. The crystals were then identified using various techniques (Figure 6 and Figure 7). The X-ray diffraction and Raman spectra reveal that the crystals grown on the SAMs are of the α-form and those from solution are β-L-glutamic acid. From X-ray diffraction, It is also evident that L-glutamic acid crystallizes on the surfaces with preferential crystal growth along the <111> crystal plane. It is also clear from the SEM images that the polymorphs possess very different crystal habits. Crystals grown on the SAM surfaces reveal well-ordered large prismatic structures typical of α-L-glutamic acid, whereas crystals from solution expose plate like structures characteristic of the β-form. These results verify the stabilization of the α-polymorph of L-glutamic acid on the L-phenylalanine terminated SAM. The stabilization is explained in the following manner: β-L-glutamic acid emerges from the (011) plane of α-L-glutamic acid. L-Phenylalanine attaches to the (011) plane of the α-crystals, thereby inhibiting and preventing the α to β transformation.

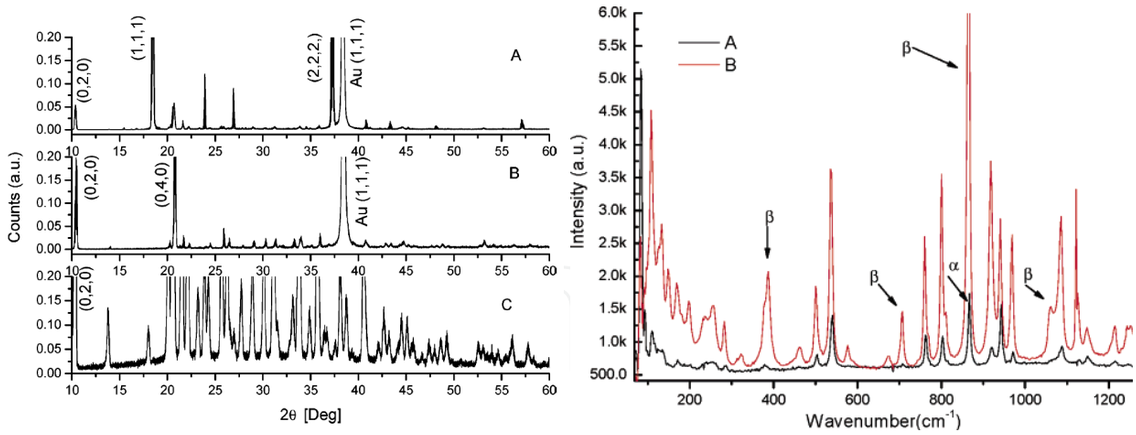


Fig. 6. X-ray diffraction of L glutamic acid crystals (A) grown on L-AAPP SAMs, (B) grown on Au and (C) grown from solution – (left) and Raman spectroscopy of L glutamic acid crystals (A) grown on L-AAPP SAMs (α-polymorph) and (B) grown from solution (β-polymorph). (Dressler and Mastai, 2007)

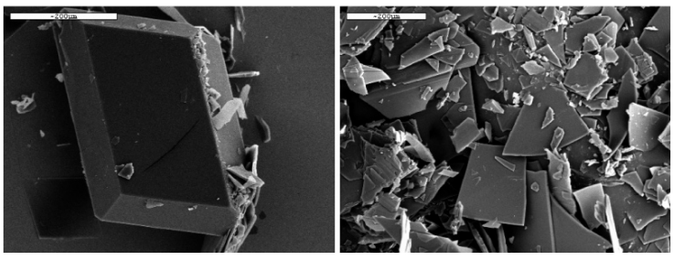

Fig. 7. Scanning electron microscopy images of L glutamic acid crystals (scale bar=200μm): (A) crystal morphology of crystals grown on the surface of L-AAPP SAMs and (B) crystal morphology of crystals grown from solution. (Dressler and Mastai, 2007)

Recently, Ejgenberg and Mastai demonstrated that self assembled monolayers based on S-leucine (Figure 8) can be used for polymorphism control of DL glutamic acid (Ejgenberg and Mastai, 2011). It is known that DL-glutamic acid can crystallize in two forms: the conglomerate form, known as anhydrous DL glutamic acid and the racemic compound, known as DL glutamic acid monohydrate. Ejgenberg and Mastai were able to afford anhydrous DL glutamic acid under conditions where the monohydrated DL glutamic acid is thermodynamically more stable.

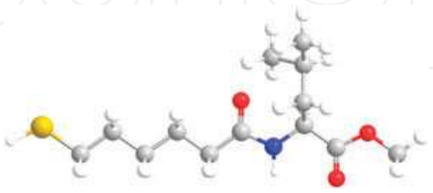

Fig. 8. S-leucine methyl ester covalently attached to 6-mercaptohexanoic acid (S-LMHA). Red atoms = oxygen, blue =nitrogen, gray = carbon, yellow = sulfur, white = hydrogen. (Ejgenberg and Mastai, 2011)

The chiral SAMs were prepared on ultra-flat gold surfaces. Gold films of 50 nm thickness were deposited on mica substrates using a high vacuum sputtering technique. The chiral

SAMs were then formed on the gold surfaces by immersing the gold substrates in 0.1M solutions of S-LMHA in ethanol overnight. In order to examine the effect of the chiral SAMs on the DL-glutamic acid crystallization, DL-glutamic acid was crystallized from aqueous solution onto the S-LMHA chiral SAMs. DL-glutamic acid was also crystallized in solution, under the same conditions. The crystals from solution and those grown on the chiral SAMs were examined using X-ray diffraction (XRD), scanning electron microscopy (SEM), micro-Raman and differential scanning calorimetry (DSC). It should be mentioned that crystallization or crystal growth did not occur on the bare gold surfaces.

The X-ray diffraction spectrum of crystals from solution is shown in Figure 9 and corresponds to monohydrated DL-glutamic acid, namely the racemic compound, as reported in the literature. The monohydrate of DL-glutamic acid crystallizes in an orthorhombic unit cell (space group Pbca) with the following parameters a=9.08, b = 15.40, c = 10.61 (A˚) and $\alpha = \beta = \lambda = 90°$. On the other hand, the X-ray diffraction patterns of crystals grown on S-LMHA that were taken directly on the chiral surface show a typical X-ray diffraction spectrum of the conglomerate, anhydrous DL-glutamic acid. The X-ray diffraction spectrum of conglomerate DL-glutamic acid corresponds to that reported in the literature with unit cell parameters (in A˚): a=5.16, b=17.30, c=6.95, $\alpha = \beta = \lambda = 90°$ (orthorhombic unit cell, space group P212121).

The anhydrous and monohydrated forms of DL-glutamic acid have different crystal habits and therefore their formation was also studied using SEM. Figure 9 displays SEM images of crystals collected from solution and crystals grown on the S-LMHA SAMs. The crystals

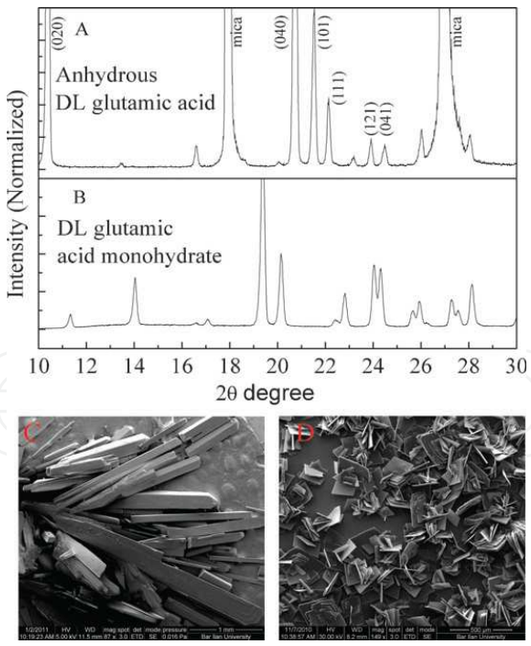


Fig. 9. X-Ray diffraction spectra of (A) DL-glutamic acid crystals grown on S-LMHA chiral SAMs (anhydrous DL-glutamic acid) and (B) crystals grown in solution (DL-glutamic acid monohydrate) and SEM images of (C) crystals grown in solution (scale bar = 1 mm) (DL-glutamic acid monohydrate) and (D) crystals grown on S-LMHA chiral SAMs (scale bar = 500 mm) (anhydrous DL-glutamic acid). (Ejgenberg and Mastai, 2011)

grown from solution reveal typical needle-like morphology, characteristic of monohydrated DL-glutamic acid. The crystals are fairly large and non-uniform in size (1–4 mm long and 0.2–0.5 mm wide). However, crystals grown on the S-LMHA SAMs expose plate like morphology characteristic of anhydrous DL-glutamic acid. They are uniform in size with approximately 250 X 250 μm² and are much smaller than the crystals from solution.

In order to further characterize the conglomerate and racemic compound DL-glutamic acid crystals, micro-Raman measurements were carried out. The Raman spectrum of DL-glutamic acid crystallized on the S-LMHA surface is shown in Figure 10 with main peaks at 867, 1295, 1339 and 1405 cm–1. The Raman spectrum of DL-glutamic acid crystallized from solution (Figure 10) displays main peaks at 855, 919 and 1314 cm–1. These spectra correspond to the Raman spectra of conglomerate and racemic glutamic acid as reported in the literature. The Raman measurements of DL-glutamic acid crystallized on the chiral surface match those of the conglomerate form of DL-glutamic acid.

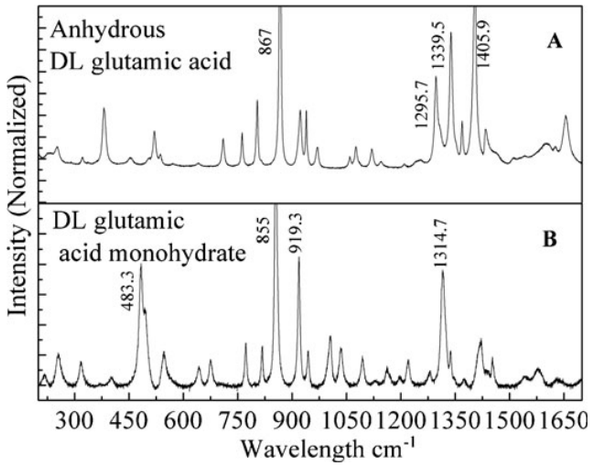


Fig. 10. Raman spectra of (A) DL-glutamic acid crystals grown on S-LMHA chiral SAMs (anhydrous DL-glutamic acid) and (B) crystals grown in solution (DL-glutamic acid monohydrate). (Ejgenberg and Mastai, 2011)

Further evidence for the formation of the conglomerate DL-glutamic acid crystals on the chiral SAM surfaces was obtained from differential scanning calorimetry (DSC) (Figure 11). The DSC thermogram of the DL-glutamic crystals grown on the S-LMHA SAMs exhibits a sharp melting point at 185.4 1C. The DSC thermogram of the crystals from solution shows two endothermic peaks at 112.7 1C and 184.7 1C. These results can be explained in the following manner. The crystals grown on the chiral SAMs are anhydrous DL-glutamic acid and therefore exhibit one peak, while those from solution are monohydrated DL-glutamic acid and therefore contain two peaks: the first endotherm is due to the loss of water molecules and the second sharp endotherm is due to the melting of anhydrous DL-glutamic acid.

In conclusion, S-LMHA SAMs were used to stabilize the conglomerate form of DL-glutamic acid crystals. The results offer a powerful tool in the development of processes for controlling chiral polymorphic systems and can further develop into a novel method for chiral resolution by crystallization.

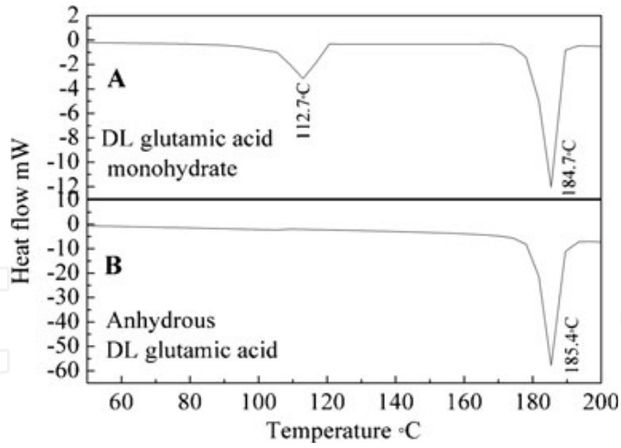


Fig. 11. DSC thermograms of (A) DL-glutamic acid crystals grown in solution (DL-glutamic acid monohydrate) and (B) crystals grown on S-LMHA chiral SAMs (anhydrous DL-glutamic acid). (Ejgenberg and Mastai, 2011)

### 2.3 Crystallization on patterned SAMs

Patterned SAMs are composed of two or more SAMs which are deliberately distributed on specific areas on the surface. They can be fabricated in different ways including micro-contact printing and dip-pen nanolithography. Patterned SAMs have been used to attract particular nanostructures like ribbons or wires to particular areas on the surface. They have also been used in the functionalization of biosensors in which the localized SAMs have an affinity for specific cells and proteins. Crystallization on patterned SAMs where the crystals grow in localized areas has also been demonstrated.

In a fascinating study, Aizenberg *et al.* demonstrated that crystallization could be restricted to well-defined regions on micro-patterned SAMs (Aizenberg *et al.*, 1999). The substrates were used in order to control the crystallization of calcite. Calcite is a stable polymorph of calcium carbonate, with space group R3c, α = 4.99Å and c = 17.06Å. Calcite has been extensively studied and its crystallization is relatively easy to perform.

Self assembled monolayers having areas of different nucleating activity were patterned on metal substrates. The self assembled monolayers were patterned by microcontact printing with an elastomeric stamp that had a relief structure consisting of a square array of raised circles: as inks, 10mM solutions of $HS(CH_2)nX$ ($X=CO_2H$) in ethanol were used. The surface was then washed with a 10mM solution of $HS(CH_2)_{15}CH_3$ in ethanol to passivate the areas that had not contacted the stamp. The patterned substrates were supported upside down in the crystallizing solutions to ensure that only particles grown on the SAM would be bound to the surface.

Figure 12 shows a low magnification image of calcite crystals formed on one of the patterned SAMs. It is clear that crystallization is restricted to well defined, $CO_2$ – terminated regions and does not occur on the $CH_3$ – terminated areas. Interestingly, by adjusting parameters such as the density and size features on the stamp, Aizenberg *et al.* could control important crystallization characteristics, including the location and density of nucleating regions on the surface, the number of crystals nucleated in each region and the crystallographic orientation of the crystals (Figure 13). The following mechanism was suggested: the rate of nucleation on SAMs

terminated in polar groups is faster than on methyl-terminated SAMs. As soon as crystal growth begins in a polar region, mass transport to the growing crystals depletes calcium and carbonate ions over the local methyl-terminated region to the point of under saturation.

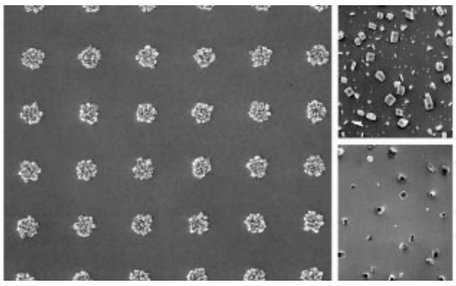

Fig. 12. Scanning electron micrograph of a patterned surface – calcite crystals appear on circles of $HS(CH_2)_{15}CO_2H$ in a background of $HS(CH_2)_{15}CH_3$. (Aizenberg *et al.*, 1999)

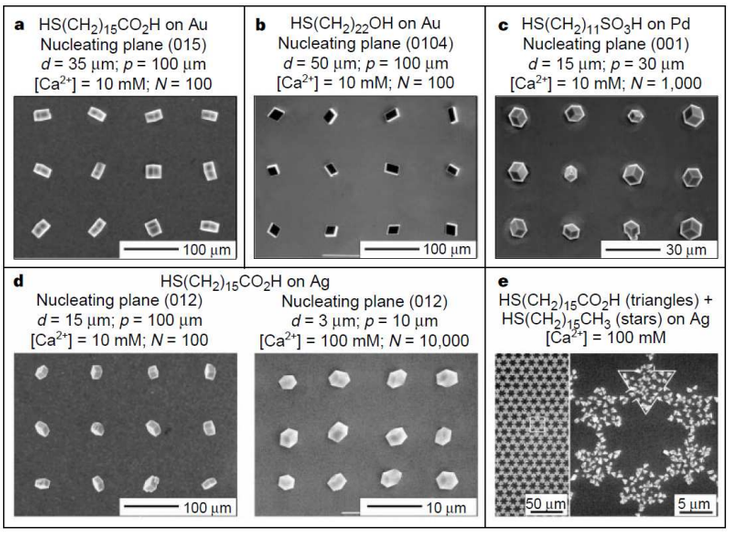


Fig. 13. Ordered two dimensional arrays of calcite crystals. (Aizenberg *et al.*, 1999)

Recently, Lee *et al.* investigated the concomitant crystallization of glycine polymorphs on patterned self assembled monolayers (Lee, I.S. *et al.*, 2008). Six distinct polymorphic forms of glycine are known in the literature; three of them – α, β and γ - are formed at ambient environment. At room temperature, γ-glycine is the thermodynamically most stable form. However, in neutral aqueous solution, the α-form is normally obtained. The γ-form is typically obtained from acidic and basic solutions. β-glycine is the least stable of the three forms. It can be obtained from ethanol-water mixtures, but readily converts to α-glycine in the presence of water or upon heating.

Patterned subtrates were designed in the following manner: metallic gold islands were formed by evaporating titanium followed by gold through brass meshes onto glass substrates. The dimensions and patterns of the islands depended on the size and shape of the holes on the mesh. Square shaped islands in a variety of sizes were prepared. 4-Mercaptobenzoic acid (4-MBA) was self assembled onto the gold surface while octadecyltrichlorosilane (OTS) was applied to the exposed glass surface.

The crystallization experiments were conducted by immersing and withdrawing the patterned substrates from aqueous glycine solutions of three different pHs (neutral, acidic and basic) and concentrations. Solution droplets were created on the patterned surface and each droplet served as an independent crystallization trial. More than 2000 islands per substrate were analyzed to achieve the statistical accuracy of the polymorph distribution of crystals formed on the substrate.

| pH | concentration (M) | size of island ($\mu$m) | total samples | crystallization time (min)[a] | α-form (%) | $\beta$-form (%) | $\gamma$-form (%) |
|---|---|---|---|---|---|---|---|
| 3.40 | 1.60 | 500 | 2000 | 8 | 36.3 | 0.4 | 63.3 |
| | 2.40 | 500 | 2000 | not measured | 54.1 | 10.4 | 35.5 |
| | 3.20 | 500 | 2000 | 25 | 66.0 | 7.8 | 26.2 |
| 5.90–6.20 | 1.60 | 500 | 2000 | 5 | 90.3 | 7.3 | 2.4 |
| | 2.40 | 500 | 2000 | 5 | 88.3 | 5.8 | 5.9 |
| | 3.20 | 500 | 3000 | 10 | 92.2 | 2.9 | 4.9 |
| 10.10 | 1.60 | 500 | 2000 | 100 | 58.2 | 6.4 | 35.4 |
| | 2.40 | 500 | 2000 | 220 | 68.2 | 10.3 | 21.5 |
| | 3.20 | 500 | 2000 | 450 | 83.8 | 4.9 | 11.3 |

[a] The crystallization time corresponds to the time when crystals are observed on 99% islands of the patterned substrate.

Table 2. Polymorph distribution of glycine for different pHs and solution concentrations. (Lee, I.S. *et al.*, 2008)

The polymorph distribution of glycine crystals formed on the patterned substrates with respect to the solution concentration and pH are summarized in Table 2. For the neutral aqueous glycine solution, the α-form was preferred at all concentrations, but its frequency significantly decreased at acidic and basic solutions. Consequentially, the percentage of γ-glycine increased in the acidic and basic solutions, without any large difference in the polymorph distribution of the β-polymorph. The increased percentage of the γ-polymorph in acidic and basic solutions was rationalized in the following way: the acidic and basic glycine solutions contain charged glycine species which reduce the possibility of the formation of α-glycine. Table 3 summarizes the polymorph outcome of glycine for different pHs and island sizes. As shown in previous reports (Lee, A.Y. *et al.*, 2005, 2006), metastable forms (β-glycine) were consistently more frequently observed with smaller islands. However, using acidic and basic glycine solutions, the frequency of the thermodynamically most stable γ-glycine increased with decreasing island size. This can be attributed to the increased proportion of the charged glycine species caused by the decrease/increase in the pH of solution for acidic/basic solutions during evaporation.

| pH | concentration (M) | size of island ($\mu$m) | total samples | crystallization time (min)[a] | α-form (%) | $\beta$-form (%) | $\gamma$-form (%) |
|---|---|---|---|---|---|---|---|
| 3.40 | 3.20 | 250 | 3000 | 10 | 11.6 | 14.1 | 73.3 |
| | | 500 | 2000 | 25 | 66.0 | 7.8 | 26.2 |
| 5.90–6.20 | 3.20 | 250 | 3000 | 5 | 94.5 | 5.4 | 0.1 |
| | | 500 | 3000 | 10 | 92.2 | 2.9 | 4.9 |
| 10.10 | 3.20 | 250 | 2000 | 60 | 52.4 | 17.1 | 30.5 |
| | | 500 | 2000 | 450 | 83.8 | 4.9 | 11.3 |

[a] The crystallization time corresponds to the time when crystals are observed on 99% islands on the substrate.

Table 3. The polymorph outcome of glycine for different pHs and island sizes. (Lee, I.S. *et al.*, 2008)

In similar studies, Lee *et al.* reported that the size of the glycine crystals is controlled by the dimensions of the metallic gold islands or the concentration of the solution (Lee, A.Y. *et al.*, 2005). Moreover, it was observed that the high energy unstable β-form of glycine crystallizes

on small metallic islands, in contrast to large islands, where the α-form is favoured. The increased frequency of the high energy form (β-glycine) with decreasing feature sizes is a result of the high supersaturation that is generated from fast solvent evaporation. (Lee, A.Y. et al., 2006)

## 3. Enantioselective crystallization

The crystallization of racemic molecules is very similar to the crystallization of achiral molecules. However, because of their chirality, racemic molecules can form different types of crystals with different compositions. If the crystal lattice contains equal left and right handed molecules arranged in an ordered manner, the crystal is heterochiral and referred to as a racemic compound. In the case where the crystal lattice is composed of only one enantiomer (left or right), the crystal is homochiral and referred to as a conglomerate. In nature, racemic compounds greatly outnumber conglomerates.

Chiral resolution is the process of the separation of racemates into their enantiomers. Many methods have been developed for this purpose. The most common is the use of chiral stationary phases in HPLC. However, large scale chiral separation is based on the classical crystallization method, which incorporates diasteriomeric transformation and chiral seeding. Even today, new methods of chiral crystallization are being designed. Lahav et al. developed a method, called "tailor-made" additives, which has been exploited for the kinetic resolution of conglomerates (Addadi, 1982). These additives have molecular structures which are very similar to one of the enantiomorphs of the substrate crystals. Consequentially, the inhibitors stereoselectively adsorb to the surfaces of one of the enantiomorphs, delaying or preventing its growth. As a result, enantiomeric excess is achieved. It is important to mention that in order to acheive chiral resolution by crystallization, the racemate system must spontaneously resolve upon crystallization to a conglomerate.

## 4. Chiral SAMs and enantioselective crystallization on chiral SAMs

As mentioned above, SAMs are organic assemblies formed by the adsorption of molecules from solution or the gas phase onto the surface of solids. If the adsorbed molecules are chiral, the self assembled monolayer is also rendered chiral. The chirality of the molecule can be distributed within the monolayer interior or located at the terminus of the molecule. However, the chirality is only expressed when the chiral constituent is exposed at the monolayer surface. Chiral SAMs are used in chiral systems. The SAMs can be used to specifically interact with chiral species, such as proteins or amino acids. Chiral SAMs have been used in enantioselective crystallization. In this case, a racemic solution of a chiral molecule is crystallized on a chiral SAM. The chiral SAM serves as a nucleating surface for one of the enantiomers, thereby increasing its crystallization on the SAM. Thus, enantioselective crystallization is achieved.

Dressler and Mastai studied the enantioselective crystallization of glutamic acid on self assembled monolayers of cysteine (Dressler and Mastai, 2007). The chiral SAMs were prepared by immersing gold covered glass slides in aqueous solutions of cysteine (10mM) for 2 hours. These SAMs were then characterized by X-ray diffraction, micro-Raman measurements, X-ray photoelectron spectroscopy, contact angle and ellipsometry.

In order to study the interactions between the chiral crystals and the chiral SAMs, pure enantiomers of glutamic acid were first crystallized on the L and D cysteine films. Interestingly, enantiomers of glutamic acid with identical chirality to that of the cysteine SAMs did not grow on the SAMs in a specific orientation and were unchanged from crystals grown in solution (Table 4). On the other hand, enantiomers with chirality opposite to that of the cysteine films grew in a preffered orientation. In either case, morphological differences between crystals grown on the SAMs and those grown in solution were not very significant.

| | (+)-L cysteine film | | -D cysteine films | | Pure solution | |
|---|---|---|---|---|---|---|
| Crystal system | Crystal habit | Crystal orientation | Crystal habit | Crystal orientation | Crystal habit | Crystal orientation |
| (+)-L glutamic acid | Plate like | No specific orientation | Plate like | [020] | Plate like | No specific orientation |
| (−)-D glutamic acid | Plate like | [020] | Plate like | No specific orientation | Plate like | No specific orientation |
| *rac*-glutamic acid | Rectangular (well oriented) | [220] | Plate like | [220] | Needle like | No specific orientation |

Table 4. Crystal habits and crystal orientation of DL, D and L glutamic acid crystallized on cysteine films and in pure solution. (Dressler and Mastai, 2007)

The chiral cysteine SAMs were then utilized for the enantioselective crystallization of glutamic acid. For this purpose, L and D cysteine SAMs were immersed in supersaturated solutions of DL-glutamic acid for ca. 2 hours. The crystals were then characterized using various techniques. It is important to note here that glutamic acid grows as a monohydrate crystal from water and therefore has a different structure from its enantiomers which were discussed previously. Figure 14 presents SEM images of glutamic acid monohydrate crystals grown on L and D cysteine surfaces and grown from solution. Crystals grown from solution have a needle-like morphology with an average size of 300 µm whereas crystals grown on the cysteine surfaces grow in well ordered arrays of rectangular/plate like shaped crystals with a typical size of 10-30 µm. X-ray diffraction measurements of the crystals showed preffered orientation of the glutamic acid crystals (Table 4).

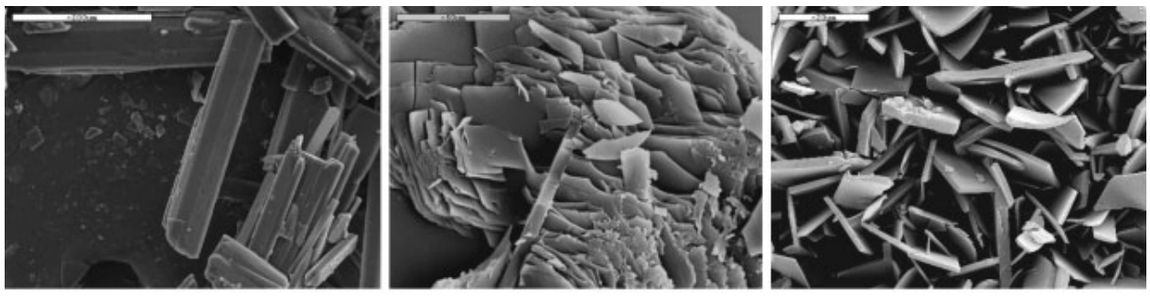

**A** (scale bar=200µm) **B** (scale bar=50µm) **C** (scale bar=20µm)

Fig. 14. SEM images featuring the crystal morphology of rac-glutamic acid crystallized (A) from solution, (B) on a chiral D-cysteine surface and (C) on a chiral L-cysteine surface. (Dressler and Mastai, 2007)

The enantiomeric excess of the crystals grown on the chiral SAMs was investigated using polarimetry. The crystals were gently removed from the chiral films, dissolved in 5N HCl

solution and their optical activity was measured. The results show that the enantiomeric excess of glutamic acid crystals collected from the L-cysteine films is about 31% e.e. enriched with D-glutamic acid (Table 5). The crystallization on the D-cysteine films resulted in 27% e.e. enriched with L-glutamic acid. The optical activity of the crystallization solution was also measured (at different intervals). The optical activity results measured from the solution and from the crystals are in good agreement with each other.

| | (+)-L cysteine film | | (−)-D cysteine film | |
|---|---|---|---|---|
| Crystal system | e.e in solution (%) | e.e of crystals on chiral surface (%) | e.e in solution (%) | e.e of crystals on chiral surface (%) |
| *rac*-glutamic acid | 15 -L after 45 min | 31 -D | 12 -D after 45 min | 27- L |

Table 5. Enantiomeric excess of crystals crystallized in solutions and on chiral cysteine surfaces. (Dressler and Mastai, 2007)

Dressler and Mastai also studied the crystallization of histidine on the chiral cysteine films. They demonstrated that the cysteine films induce a modification in histidine morphology and lead to specific orientation of the histidine crystals. They also found that the L and D cysteine surfaces were active in chiral discrimination. Again, the enantiomeric excess was ca. 30%.

Singh *et al.* used chiral self assembled monolayers (Figure 15) as resolving auxiliaries in the crystallization of valine (Singh *et al.*, 2010). When starting with racemic solutions, the crystals obtained on the chiral SAMs contained one of the valine enantiomers in excess. The enantiomer obtained in excess was always of opposite chirality to the monolayer used. The chiral resolution was enhanced as a result of decreasing supersaturation. In addition, Singh et. al also monitored the crystallization of valine on chiral SAMs beginning with initial solutions containing one of the enantiomers in excess. When starting with a solution containing 50% ee, crystals of one pure enantiomer were obtained on the SAMs whereas mixtures of the pure enantiomer and the racemic compound were obtained in control experiments, not containing the chiral SAMs. The enantiomer obtained on the chiral SAMs was the enantiomer initially present in excess, regardless of the chirality of the monolayer being used.

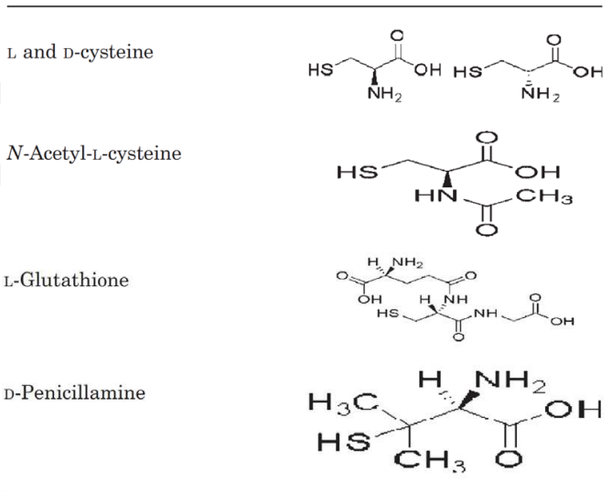


Fig. 15. Chemical structures of the chiral self assembled monolayers. (Singh *et al.*, 2010)

Banno *et al.* studied the enantioselective crystal growth of leucine on self assembled monolayers with covalently attached D or L-leucine molecules (Banno *et al.*, 2004). The monolayers were formed in the following way: gold substrates were prepared by vapour deposition of gold on quartz crystals. The substrates were flame annealed and subsequently immersed in 2 mM ethanolic solutions of 11-mercaptoundecanoic acid (MAU). Leucine was then covalently attached to the MAU monolayer. The crystals on the SAM were grown by immersing the substrates in saturated solutions of D, L or DL-leucine.

In order to identify the leucine crystals grown on the monolayers, X-ray diffraction and QCM (quartz crystal microbalance) measurements were utilized. Figure 16 shows XRD patterns of the leucine SAMs after immersion in a 175 mM D or L-leucine solution for 3 hrs. For the D-leucine SAM, the diffraction peak was observed only after it was immersed in the D-leucine solution, whereas no peak appeared when it was immersed in the L-leucine solution. With the L-leucine SAM, exactly the opposite results were obtained. The diffraction angles of the two observed peaks were identical to eachother and equal to 6.07°. The above mentioned cross inversion between D and L-leucine strongly suggests that the crystallization on the Leucine SAM is highly enantioselective. The enantioselectivity was also confirmed by the increase in surface mass resulting from the grown leucine crystals on the modified SAM, detected by QCM.

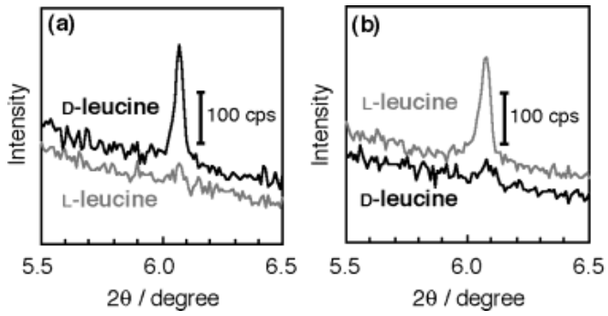


Fig. 16. XRD patterns of (a) D and (b) L-leucine SAMs after immersion in pure enantiomeric leucine solutions. (Banno *et al.*, 2004)

The leucine monolayers were also immersed in saturated DL-leucine solutions. As shown in Figure 17, a diffraction peak was observed at 6.34° for both D and L-leucine SAMs. This happens because in the presence of equimolar amounts of D and L enantiomers of leucine, the racemic crystal tends to form instead of either one of the two pure enantiomeric crystals.

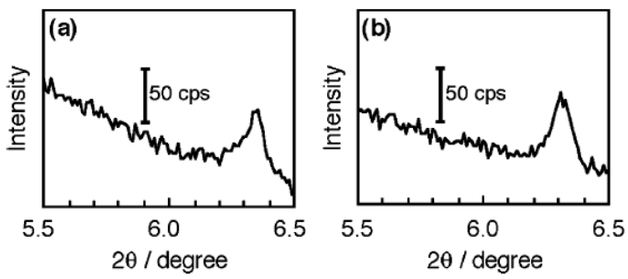


Fig. 17. XRD patterns of (a) D and (b) L-leucine SAMs after immersion in racemic leucine solution. (Banno *et al.*, 2004)

It should be noted that the primary interaction between the enantiomers attached on the SAMs and prenucleation aggregates formed in solution is due to hydrophobic bonding or Van der Waals interaction. It is assumed that crystal growth proceeds only when the chirality of the prenucleation aggregate of pure enantiomers formed in solution is the same as that of the attached enantiomer. In racemic solution, on the contrary, most of the prenucleation aggregates are considered to be in DL-form, resulting in the growth of the racemic crystalline phase on both D and L-leucine attached SAMs.

## 5. Conclusions

In this book chapter the preparation, structure, properties and applications of self-assembled monolayers (SAMs) in crystallization processes have been briefly reviewed. We have reviewed a variety of applications of SAMs in crystallization which can be catalogued into either pure crystallization methods or through the expression of chiral molecular interactions of SAMs.

Although two decades have passed since the discovery of SAMs, it is still a very active and broad research area that is almost impossible to review comprehensively. The fundamental questions of adsorption, structure, phases, and phase transitions have been thoroughly studied in the past, but still several issues remain unresolved. A large part of present and future work is aimed at the modification and fictionalization of surfaces by SAMs for different applications, with molecular and biological recognition being the most dynamic. Since SAMs are not so much a specific class of compounds, but rather a very flexible concept with virtually unlimited potential for applications, we expect that the area of SAMs will continue to prosper.

## 6. Acknowledgment

M. Ejgenberg would like to acknowledge the BIU President's scholarship and the ministry of science and technology program for the promotion of women in science and technology for funding.

## 7. References

Addadi, L., Weinstein, S., Gati, E., Weissbuch, I., & Lahav, M. (1982). Resolution of conglomerates with the assistance of tailor-made impurities. Generality and mechanistic aspects of the "rule of reversal". A new method for assignment of absolute configuration. *Journal of the American Chemical Society*, Vol. 104, 4610-4617

Aizenberg, J., Black, A.J., & Whitesides, G.M. (1999). Control of crystal nucleation by patterned self-assembled monolayers. *Letters to Nature*, Vol. 398, 495-498

Aizenberg, J., Black, A.J., & Whitesides, J.M. (1999). Oriented growth of calcite controlled by self assembled monolayers of functionalized alkane thiols supported on gold and silver. *Journal of the American Chemical Society*, Vol. 121, 4500-4509

Banno, N., Nakanishi, T., Matsunaga, M., Asahi, T., & Osaka, T. (2004). Enantioselective crystal growth of leucine on a self assembled monolayer with covalently attached leucine molecules. *Journal of the American Chemical Society*, Vol. 126, 428-429

Chieng, N., Rades, T., & Aaltonen, J. (2011). An overview of recent studies on the analysis of pharmaceutical polymorphs. *Journal of Pharmaceutical and Biomedical Analysis*, Vol. 55, 618–644

Chun, K.Y., & Stroeve, P. (2002). Protein Transport in Nanoporous Membranes Modified with Self-Assembled Monolayers of Functionalized Thiols. *Langmuir*, Vol. 18, 4653-4658

Dressler, D.H. & Mastai, Y. (2007). Chiral crystallization of glutamic acid on self assembled films of cysteine. *Chirality*, Vol. 19, 358-365

Dressler, D.H., & Mastai, Y. (2007). Controlling polymorphism by crystallization on self assembled multilayers. *Crystal Growth & Design*, Vol. 7, No. 5, 847-850

Eckermann, A.L., Feld, D.J., Shaw, J.A., & Meade, T.J. (2010). Electrochemistry of redox-active self-assembled monolayers. *Coordination Chemistry Reviews*, Vol. 254, 1769-1802

Ejgenberg, M. & Mastai, Y. (2011). *Chemical Communications*, DOI: 10.1039/c1cc14952k.

Garti, N. & Zour, H. (1997). The effect of surfactants on the crystallization and polymorphic transformation of glutamic acid. *Journal of Crystal Growth*, Vol. 172, 486-498

Hiremath, R., Basile, J.A., Varney, S.W., & Swift, J.A. (2005). Controlling molecular crystal polymorphism with self assembled monolayer templates. *Journal of the American Chemical Society*, Vol. 127, No. 51, 18321-18327

Lee, A.Y., Ulman, A., & Myerson, A.S. (2002). Crystallization of amino acids on self assembled monolayers of rigid thiols on gold. *Langmuir*, Vol. 18, 5886-5898

Lee, A.Y., Lee, I.S., Dette, S.S., Boerner, j., & Myerson, A.S. (2005). Crystallization on confined engineered surfaces: a method to control crystal size and generate different polymorphs. *Journal of the American Chemical Society*, Vol. 127, 14982-14983

Lee, A.Y., Lee, I.S., & Myerson, A.S. (2006). Factors affecting the polymorphic outcome of glycine crystals constrained on patterned substrates. *Chemical Engineering and Technology*, Vol. 29, No. 1, 281-285

Lee, I.S., Kim, K.T., Lee, A.Y., & Myerson, A.S. (2008). Concomitant crystallization of glycine on patterned substrates: the effect of pH on the polymorphic outcome. *Crystal Growth & Design*, Vol. 8, No. 1, 108-113

Love, J.C., Estroff, L.A., Kriebel, J.K., Nuzzo, R.G. & Whitesides, G.M. (2005). Self assembled monolayers of thiolates on metals as a form of nanotechnology. Chemical Reviews, Vol. 105, No. 4, 1103-1169

Mastai, Y. (2009). Enantioselective crystallization on nanochiral surfaces. *Chemical Society Reviews*, Vol. 38, 772-780

Nyquist, R.M., Eberhardt, A.S., Silks III, L.A., Li, Z., Yang, X., & Swanson, B.I. (2000). Characterization of self-assembled monolayers for biosensor applications. *Langmuir*, Vol. 16, 1793-1800

Singh, A. & Myerson, A.S. (2010). Chiral self assembled monolayers as resolving auxiliaries in the crystallization of valine. *Journal of Pharmaceutical Sciences*, Vol. 99, 3931-3940

Smith, R.K., Lewis, P.A., & Weiss, P.A. (2004). Patterning self assembled monolayers. *Progress in surfaces science*, Vol. 75, 1-68

Ulman, A. (1996). Formation and structure of self assembled monolayers. *Chemical Reviews*, Vol. 96, 1533-1554

Weissbuch, I., Torbeev, V.Y., Leiserowitz L., & Lahav, M. (2005). Solvent effect on crystal polymorphism: Why addition of methanol or ethanol to aqueous solutions induces

the precipitation of the least stable β form of Glycine. *Angewandte Chemie International Edition*, Vol. 44, 3226-3229

Yokota, M., Doki, N., & Shimizu, K. (2006). Chiral separation of a racemic compound induced by transformation of racemic crystal structures: DL-Glutamic acid. *Crystal Growth & Design*, Vol. 6, No. 7, 1588-1590

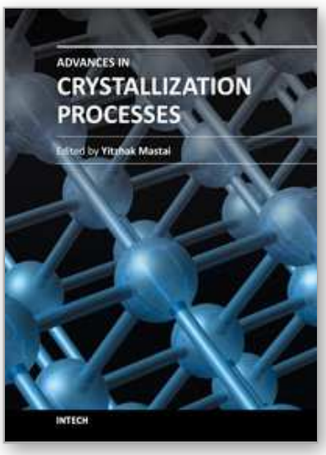


**Advances in Crystallization Processes**

Edited by Dr. Yitzhak Mastai

ISBN 978-953-51-0581-7
Hard cover, 648 pages
**Publisher** InTech
**Published online** 27, April, 2012
**Published in print edition** April, 2012

Crystallization is used at some stage in nearly all process industries as a method of production, purification or recovery of solid materials. In recent years, a number of new applications have also come to rely on crystallization processes such as the crystallization of nano and amorphous materials. The articles for this book have been contributed by the most respected researchers in this area and cover the frontier areas of research and developments in crystallization processes. Divided into five parts this book provides the latest research developments in many aspects of crystallization including: chiral crystallization, crystallization of nanomaterials and the crystallization of amorphous and glassy materials. This book is of interest to both fundamental research and also to practicing scientists and will prove invaluable to all chemical engineers and industrial chemists in the process industries as well as crystallization workers and students in industry and academia.



**InTech Europe**
University Campus STeP Ri
Slavka Krautzeka 83/A
51000 Rijeka, Croatia
Phone: +385 (51) 770 447
Fax: +385 (51) 686 166
www.intechopen.com

**InTech China**
Unit 405, Office Block, Hotel Equatorial Shanghai
No.65, Yan An Road (West), Shanghai, 200040, China
中国上海市延安西路65号上海国际贵都大饭店办公楼405单元
Phone: +86-21-62489820
Fax: +86-21-62489821

IntechOpen